CHARACTERIZATION OF NOCTILUCENT CLOUDS UTILIZING A TEN-CHANNEL PHOTOMETER

Kenneth R. McKeever, Kristoffer L. Greenert, C. Russell Philbrick

Department of Electrical Engineering, The Pennsylvania State University, University Park, PA 16802, USA,
Email: krm223@psu.edu, klg260@psu.edu, crp3@psu.edu

ABSTRACT

On July 1, 2006, the ESPRIT rocket payload was launched at 0639 UTC from the Andøya Rocket Range in Andenes, Norway. At the time of launch, a strong noctilucent cloud layer was detected at 82.1 km altitude by the ALOMAR RMR LIDAR. This rocket payload was equipped with a 10-channel noctilucent cloud photometer, which included 5 pairs of two channels each. Each pair included orthogonal polarization filters and looked out of the rocket at different angles. Three wavelengths of 340 nm, 420 nm, and 550 nm were assigned to the channel pairs. This photometer was designed to allow identification of many characteristics of a noctilucent cloud layer. The different polarizations in each pair permitted examination of the polarization effects in the light scattered from noctilucent cloud particles. Three different wavelengths allow several different color ratios to be computed from the data.

1. NOCTILUCENT CLOUDS

The formation of noctilucent clouds is a polar phenomenon which occurs when water vapor freezes in the upper mesosphere, around 85 km. In the winter, gravity waves propagating upwards into the mesosphere break and provide an important heat source for the region. In the summer, however, most of the gravity wave spectrum are attenuated by stratospheric winds and remove this heat source before reaching the mesosphere. The momentum from breaking gravity waves accelerates an upward atmospheric circulation in the summer polar region that causes adiabatic cooling and transports water vapor [1]. Gravity wave momentum deposited in the mesosphere drives an upward velocity of the order of 10 cm/sec, resulting in adiabatic cooling. Temperatures in the mesosphere drop below 130 K, and freeze the low concentrations of water vapor, about 2 to 5 ppm .

The frequency and intensity of noctilucent cloud formations can be a useful indicator of chemical and thermodynamic effects occurring in the middle atmosphere. For example, additional water transport, and/or enhanced methane oxidation reactions in the stratosphere can result in water vapor increases, which may lead to brighter and more frequent noctilucent clouds. The study of noctilucent clouds offers potential advantages in detecting changes in our environment.

Noctilucent clouds (NLCs) are composed of small particles of ice which can be found in the upper mesosphere, about 80 to 85 km altitude. During the polar summer, such clouds form in northern and southern polar latitudes. The clouds are visible when the sun shines over the pole of the Earth, illuminating the clouds for an observer on the night side of the Earth, see Fig. 1.

The exact processes for formation of the nucleation centers of noctilucent cloud particles are not fully understood. One theory is that meteoric dust provides a nucleation center for water molecules to build upon and form small ice crystals [2]. Another is that instead ions from the D region ionosphere provide the nucleation center for the particles [3]. Either way, NLC particle formation begins with a nucleation center particle, which then accumulates water molecules.

The cold temperature of the summer mesosphere is a key factor in the freezing of water molecules and growing ice crystals from water vapor concentrations of about 2 to 5 ppm. The temperature must be low enough to form ice at the low vapor pressure present at the high altitude. In previous rocket campaigns, the temperature in the summer polar mesopause region has been found to be as low as 110 K [4], and is usually below 140 K in regions where NLC layers are found.

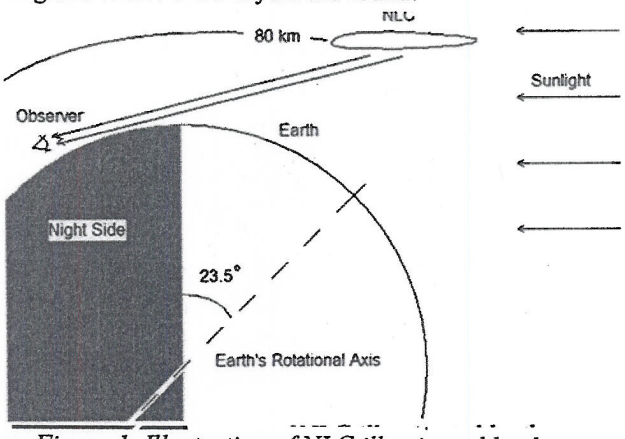

Figure 1. Illustration of NLC illuminated by the sun.

Proc.18th ESA Symposium on 'European Rocket and Balloon Programmes and Related Research', Visby, Sweden, 3-7 June 2007 (ESA SP-647, November 2007)

Tidal waves and gravity waves also play another role in causing deeper minima superimposed on the mean summer polar mesopause, and these features are apparently important in the development of noctilucent clouds, since the NLC observations tend to be located at one of these minima (for example, see [4]). However, since the density of the atmosphere decreases with increasing altitude, the gravity wave amplitude increases. When the wave reaches the area of the mesopause, temperature minima occur in response to the pressure oscillation. These features result in temperatures lower than the mean by 5 to 15 K, where NLCs and their precursors form.

NLCs provide an indicator of chemical and dynamical processes occurring in the middle atmosphere. An increase in water vapor concentration at the altitudes of NLC formation leads to brighter and more intense clouds [5]. The first noctilucent cloud sighting was recorded in 1885 after the 1883 eruption of the Krakatoa volcano in Indonesia. This large eruption contributed a huge amount of dust into the atmosphere, and possibly provided nucleation centers for NLC particles. Historical data has been tabulated in past studies [6-10] of noctilucent cloud activity. Fig. 2 shows a summary from some of the historical records.

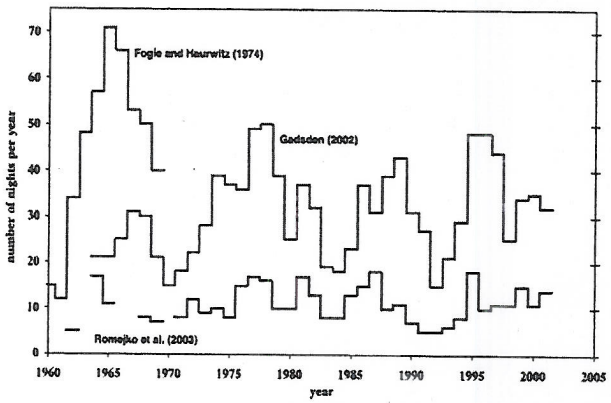

Figure 2. Frequency of NLC occurrence by year, tabulated by several authors, from [7].

2. NOCTILUCENT CLOUD PHOTOMETRY

Early investigations of noctilucent clouds made use of passive ground base imagery, and *in situ* rocket measurements using photometry. By observing sunlight scattered by noctilucent clouds, insights are gained by measuring the intensity of different wavelengths scattered from the clouds to infer density and particle size distribution [11]. Since different size particles have different light-scattering properties, photometry at multiple wavelengths provides a useful approach for studying noctilucent clouds.

Most particles in noctilucent clouds are thought to range in radius less than 20 nm; however the displays viewed by ground observers typically contain particles larger than 20 nm, since scattering $\sim r^6$. By making photometric observations in the UV and visible spectrum, between 300 to 600 nm, the properties of NLC particles can be studied. The light scattering can be described using Mie scattering theory, which provides an analytical solution to Maxwell's Equations for light scattered by spherical particles. In order for Mie scattering to be applicable to noctilucent cloud particles, the particles must be approximated by spheres. Although this is not true, it is not too unreasonable when the particles are small compared with the wavelength (other shapes have been studied by Mishchenko's group, [12]). Noctilucent cloud particles form as nucleation centers accumulate water molecules. While this process does not result in spherical particles, the resulting shape is still a good approximation when the size is small compared with the scattering wavelength.

Mie scattering is well described in Bohren and Huffman [13], which provides a computationally inexpensive method for calculating the scattering at various angles. This comparison of intensity versus different angles is referred to as a scattering phase function, and is shown in Fig. 3 for a particle size typical in bright NLCs. Since the scattering phase function depends on the radius of the particles, each particle size has a unique scattering phase function. The scattering angle dependence can be used to analyze noctilucent cloud particle sizes, if a size distribution is assumed. In noctilucent clouds, the log-normal distribution has been used to fit prior data [11].

Polarization also plays an important role in describing particle scattering using Mie theory [14, 15]. Since an electric dipole moment is induced by an incident electric field, the resulting radiation pattern varies depending on the polarization components of the incident electric field. If the sun's radiation field is separated into vertical and horizontal components, we can envision the vertical component into and out of the page in Fig. 3 resulting in the circular pattern, when viewed from above. The horizontal component vibrating in the plane of the paper results in a scattering distribution with two lobes, similar to the classic dipole field. The polarization components in the azimuth plane will radiate with nulls occurring at angles perpendicular to the direction of sun (at 90°). These differences in polarization are illustrated in Fig. 3 for a 40 nm radius particle, typical in noctilucent clouds.

3. PHOTOMETER INSTRUMENT

The noctilucent cloud photometer uses ten independent optical channels aligned with two channels in each angle position. Each channel detects light within a five-

degree field of view. The combination of each of these channels allows a total field of view of 40 degrees, as shown in Fig. 4a. Channels situated in this manner allow the instrument to make intensity measurements below, through, and above the cloud. In addition, the wide field of view would also compensate for a slight coning angle caused by payload dynamics. The instrument was mounted in the middle of the payload facing outward through an open window in the payload skin.

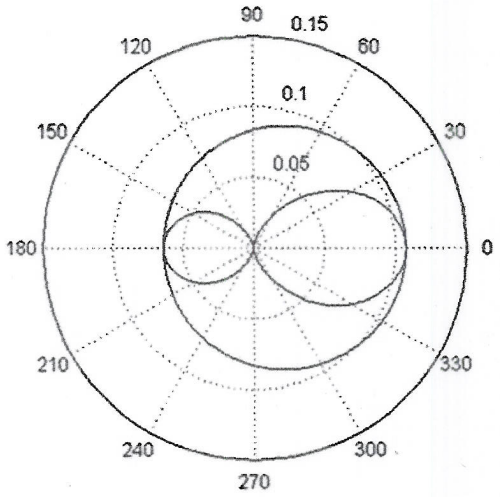

Figure 3. Mie Scattering Phase Function of 430 nm wavelength light by a 40 nm particle with parallel and perpendicular polarization

The channel numbers were assigned from left to right, then top to bottom, so that in the first row are channels 1 and 2, the second row 3 and 4, when viewing the front surface (refer to Fig. 4). Each row used the same optical filters, and each column used polarizers oriented to pass vertical E-field on left (parallel to payload axis) and horizontal direction on the right side. Fig. 4 illustrates the arrangement of filters and polarizer directions. By placing the polarizers in this manner, a ratio of intensity versus polarization angle is obtained for the same angle. Each channel consisted of a band-pass interference filter and a polarizer. Each filter had a full-width half-maximum bandwidth of about 20 nm. Three different wavelengths were flown: 340 nm, 420 nm, and 550 nm. The 420 nm filters were located in channels 1, 2, 9 and 10 to allow comparison between the upward facing and downward facing channels. Channels 3 and 4 used 340 nm filters and channels 7 and 8 used 550 nm filters. The middle two channels were flown with no filters or polarizers. Attached to the left side of the photometer was a sun sensor experiment, which provided the angle of the sun with respect to the rocket axis. The advantage of fixing the sun sensor to the photometer was the ability to easily determine the scattering angle of the sunlight, since both experiments were in the same frame of reference.

4. PRELIMINARY RESULTS

4.1. Overview

The ESPRIT payload was launched on 1 July, 2006 from the Andøya Rocket Range at 0639 UTC after the detection of strong noctilucent clouds. The NLC layer was found to exist from 81.9 to 84 km. After all payload deployments, the spin rate settled at 5.45 Hz, which provided more than five measurements of the scattering phase function every second. During the flight, coning was exhibited by the payload, with a half angle of 7.5° and a period of about 4 seconds.

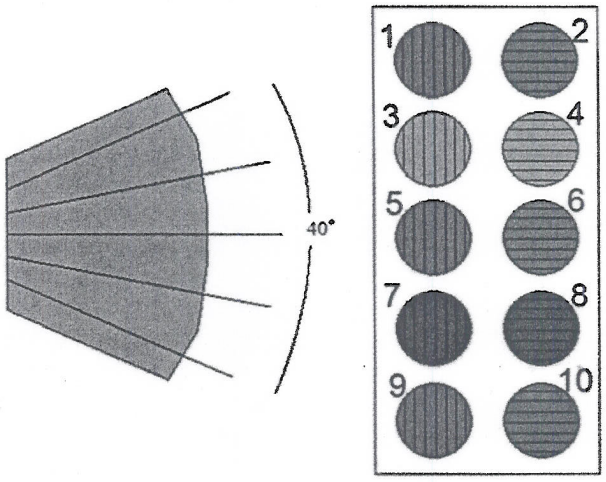

Figure 4. Photometer instrument layout from the side and front.

Channels 1 through 4 (420 nm filters and 340 nm filters) provided useful data. The channels with downward looking angles were saturated due to the Earth albedo signal. The upward looking channels were also saturated during the portion of the rotation within approximately 60 degrees of the sun. There was good dynamic contrast when the detectors were pointed at larger angles with respect to the sun and at elevations above the Earth limb. In retrospect, these problems could have been minimized with a better design in the optical baffle arrangement and with using just upward pointing photometers.

4.2. Intensity Measurements

In order to glean information about the noctilucent clouds, it is important to know the angle between the sun and the view direction of the photometer channel under analysis. This angle determines the scattering phase function – an angular measure of the scattered intensity. The orientation of the rocket was used to convert from an intensity measured versus time to an intensity measured versus angle. A first-order estimation of the angle of the detector with respect to the sun was provided by the onboard sun sensor.

Comparing lower altitude intensity centered in a region surrounding the noctilucent cloud layer with higher altitude intensity data did not show any easily recognizable differences between the two sets of data. In Fig. 5, the upper plot shows data from an altitude of 144.6 km compared to data from an altitude of 75.9 km, where the detector looked upward into the NLC layer from below. There are strong similarities between the data, so a method was needed to clearly observe differences. This was accomplished by modeling the high altitude intensity data when the rocket is well above the atmospheric scattering and the noctilucent cloud layer, and subtracting that from the lower altitude data. By doing this, it became easier to observe the variations due to the cloud layer.

Fig. 6 shows pairs of two plots for the scattering phase function at 75.9 km altitude in visible (420 nm) and ultraviolet (340 nm) wavelengths. The two plots on the left show the original data from that region, and those on the right show that data with the high altitude background intensity model subtracted. An artifact of the steep edge in the scattering of sunlight by the baffle tubes remains in the region around 60°. In Fig. 6, the scattering from NLC particles is evident at angles between 120° and 160°, as the instrument points in the northwest direction. In Fig. 5 and 6, the solid lines represent the increasing angles relative to the sun line and the dash represents decreasing angles (RH spin).

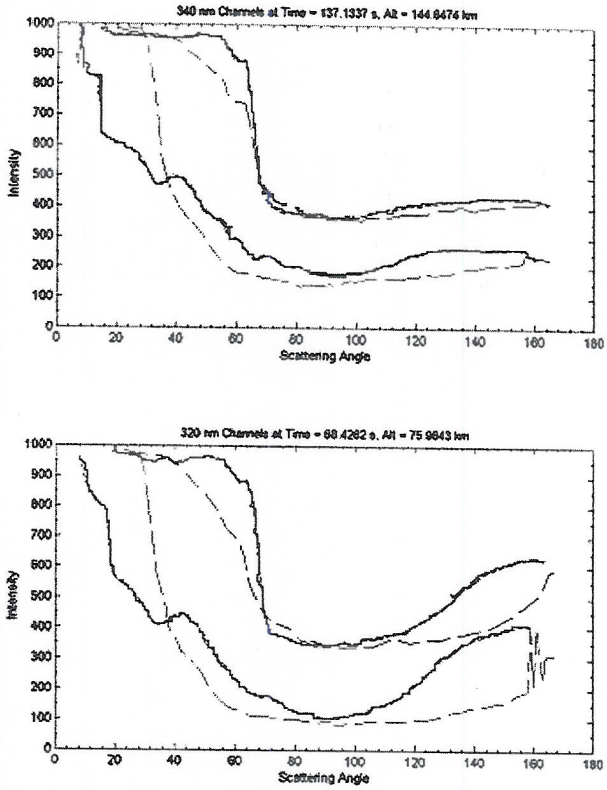

Figure 5. Comparison of data high above the NLC layer (144.6 km) with lower data below (75.9 km)

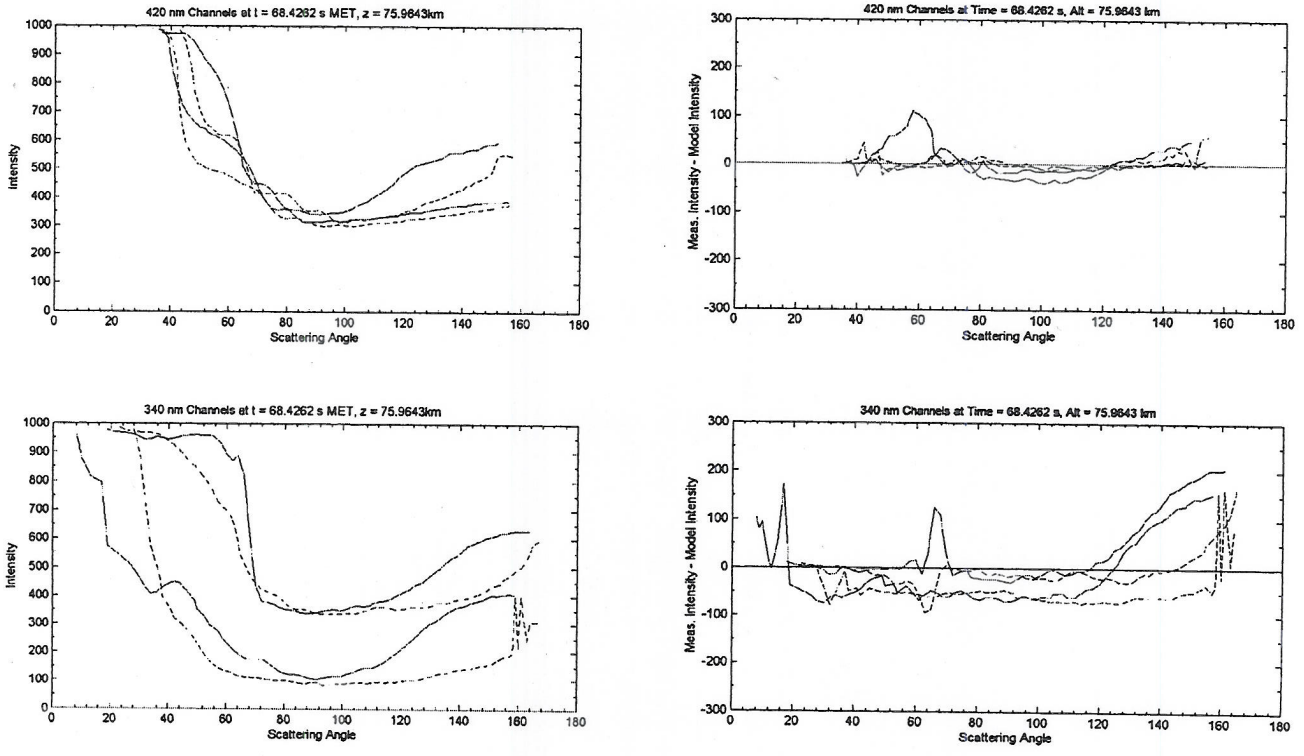

Figure 6. Photometer data for the 420 and 350 nm channels at 75.9 km before (left) and after (right) removing the modeled variation of the cone angle and the sunlight scattering in the baffle using data from high-altitude background.

4.3. Detector Path Length in NLC

The scattered light received by the detectors depends directly on the number and size of scattering particles visible to each detector. Therefore, the visible path length through the noctilucent cloud layer is important for analysis. An illustration of this path length is shown in Fig. 7, where the altitudes of the rocket and noctilucent cloud layer as well as the angle of the detector with respect to the nadir are known. The rocket trajectory, sun sensor data, and the altitude of the noctilucent cloud layer from the LIDAR measurements provide the needed information.

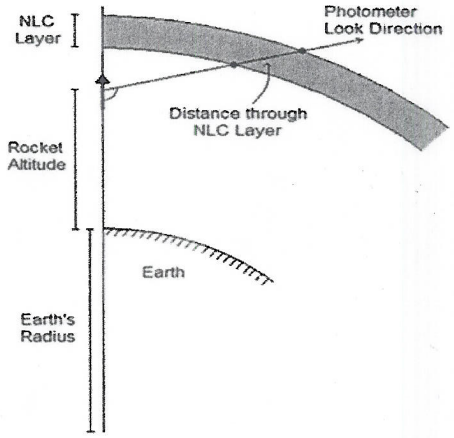

Figure 7. Geometry setup for determining path length through a noctilucent cloud layer

Information about the NLC layer was received from ALOMAR RMR LIDAR data and its presence is verified *in situ* by the photometer data. The left half of Fig. 8 shows the intensity observed by the UV detector channels as a function of altitude for the 145° scattering angle. A decrease in the intensity in the local maxima of the intensity curve is observed as the rocket ascends through the 80 to 90 km region. The intensity decreases significantly as the rocket has passes through the NLC layer.

An interesting feature also seen in Fig. 8 is the periodic increase and decrease of the intensity as the rocket ascends. This is due to the payload coning which was inherent in the payload motion during flight. Since the photometer points mostly along the azimuth plane of the rocket, detection of noctilucent clouds is hindered by the payload coning because the NLC lies in a plane nearly parallel with the detectors. The plot on the right half of Fig. 8 indicates the angle of the detector to the horizontal plane above the Earth.

As can be seen from the two plots in Fig. 8, the intensity maxima occur close to the local minima of the angle, which is associated with the coning. The data on the left of Fig. 8 is taken at a 145° scattering angle with respect to the sun, however the spatial orientation of this angle changes over time with the coning of the payload, resulting in the variation seen in the intensity as the rocket ascends.

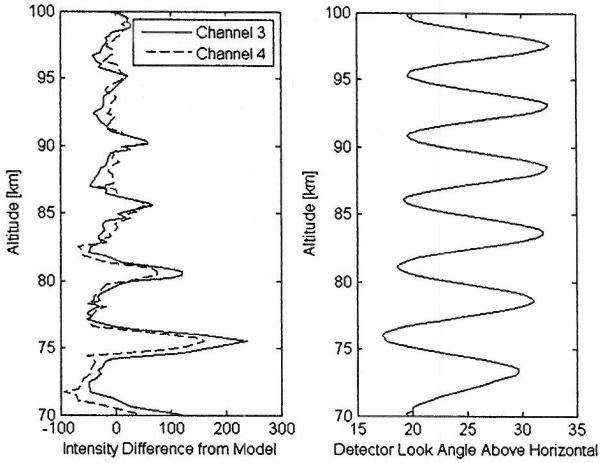

Figure 8. Intensity (left) and detector look angle above the horizontal plane (right) versus altitude at a scattering angle of 145°

Fig. 9 shows the result of calculating the expected path length in the NLC layer versus altitude. It is noted that the structure of this path length is very similar to the photometer data, Maxima and minima appear at the same altitudes, which indicates that the heights of the NLC layer determined by the LIDAR system fit the observed *in situ* data.

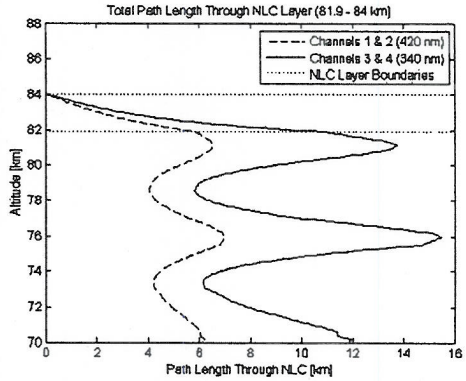

Figure 9. Detector path length through NLC layer as a function of altitude

Another issue which posed a barrier to proper analysis is the spatial geometry of the noctilucent cloud. The LIDAR detected the noctilucent cloud at an altitude of 81.9 to 84 km, but that only provides data at one point in the area where the laser illuminates the cloud. The rocket may not be passing through the same region of the cloud. These measurements show that the cloud is off to one direction based upon the azimuth (relative to the sun direction) of the scattering intensity in Fig. 10. Since the photometer detectors point mostly horizontally, the differences due to this structure are more apparent than if the channels had been facing in an

upward direction. Fig. 10 shows the ultraviolet (340 nm) scattered intensity as a function of spin azimuth (not scattering angle) relative to the sun (from East through North), and the missing data 0° to 15° and 340° to 360° are because of saturated signal values near the sun direction. The features near 60° and 300° are artifacts due to the large signal changes due to sunlight scatter from the edge of the baffle (see Fig. 6).

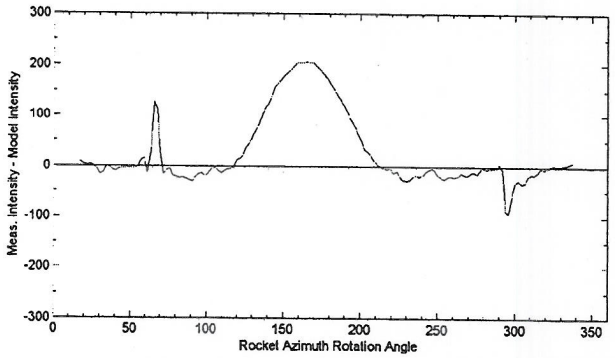

Figure 10. The residual scattered intensity just below the NLC layer show the cloud location in the northwest direction from the payload.

5. FUTURE ANALYSIS

The next task that needs to be accomplished is to complete the analysis with the instrument calibration. Once this is done and is properly applied to data, the measured intensity values will be compared on more than a qualitative basis. This will allow proper characterization of particle size, and it will allow determination of NLC layer properties, such as height and thickness, for independent comparison with ground-based LIDAR and other instruments.

This analysis is still preliminary in nature. The next priority is to determine the particle sizes within the NLC layer. In order to accomplish this, it is important to take into account the wavelength and polarization dependence. Scattering phase functions are a key to determining particle size from noctilucent cloud photometer data. The angular scattering, wavelength dependence, and polarization dependence provides an excellent way to discriminate different particle sizes and distributions. Since there are four channels of data available, these include two different wavelengths and two different polarizations, sufficient information should be available to provide accurate analysis. These analyses should then offer an opportunity for comparison with ground based measurements taken at launch. These efforts will help in validating this experiment and will result in improvements for future use of these instruments for Penn State University space projects.

6. ACKNOWLEDGEMENTS

The authors would like to acknowledge the efforts and contributions of several organizations that made this work possible. NASA Sounding Rocket Operations Contract, NASA Wallops, Andøya Rocket Range, and the RMR LIDAR at ALOMAR kindly provided the necessary launch support and resources. Funding for the project was provided by the Pennsylvania Space Grant Consortium, as well as departmental support from the College of Engineering at the Pennsylvania State University. A list of corporate sponsors can be found at http://spirit.ee.psu.edu/spiritiii/sponsers.htm.

7. REFERENCES

1. Garcia R. R., Soloman S., The effect of breaking gravity waves on the dynamics and chemical composition of the mesosphere and lower thermosphere , *J. Geophys. Res.*, Vol. 90, 3850-3868, 1985.
2. Hunten D. M., Turco R. P., Toon O. B., Smoke and dust particles of meteoric origin in the mesosphere and stratosphere, *J. Atmos. Sci.*, Vol. 27, 1342-1357, 1980.
3. Kopp E., Eberhardt P., Herrmann U., Bjorn L. G., Positive ion composition of the high-latitude summer D region with noctilucent clouds, *J. Geophys. Res.*, Vol. 90, 13,041-13,053, 1985.
4. Philbrick C. R., Barnett J., Gerndt R., Offermann D., Pendleton Jr. W. R., Witt G., Temperature measurements during the CAMP program, *Adv. Space. Res.*, Vol. 4, 153-156, 1984.
5. Thayer J. P., Rapp M., Gerrard A. J., Gudmundsson E., Kane T. J., Gravity-wave influences on Arctic mesospheric clouds as determined by a Rayleigh lidar at Sondrestrom, Greenland, *J. Geophys. Res.*, Vol. 108, PMR 17, 2003.
6. Thomas G. E., Olivero J. J., Jensen E. J., Schroeder W., Toon O. B., Relation between increasing methane and the presence of ice clouds at the mesopause, *Let. Nature*, Vol. 338, 490-492, 1989.
7. von Zahn U., Are noctilucent clouds truly a "miner's canary" for global climate change? *Eos, Trans. Amer. Geophys. Union*, Vol. 84, 261-268, 2003.
8. Fogle B., Haurwitz B., Long term variations in noctilucent cloud activity and their possible cause, *Climatological Research*, edited by Fraedrich K., Hantel M., Claussen Korff, H., Ruprecht E., Bonner Meteorologische Abhandlungen., Bonn, Germany, 263-273, 1973.
9. Gadsden M., Statistics of the annual counts of nights on which NLCs were seen, *Memoirs Brit. Astron. Assoc. Vol. 45, Mesospheric Clouds 2002*, edited by Gadsden, M., James, N. D., presented at the meeting in Perth, Scotland.
10. Romejko V. A., Dalin P. A., Pertsyev N. N., Forty years of noctilucent cloud observations near Moscow: Database and simple statistics, *J. Geophys. Res.*, Vol. 108, PMR 10, 2003.
11. Gumbel J., Stegman J., Murtagh D. P., Witt G., Scattering phase functions and particle sizes in noctilucent clouds, *Geophys. Res. Letters*, Vol. 28, 1415-1418, 2001.
12. Zakharova, N.T., M.I. Mishchenko, Scattering properties of needlelike and platelike ice spheroids with moderate size parameters, *Appl. Opt.* 39, 5052-5057, 2000.
13. Bohren C. F., Huffman D. R., *Absorption and Scattering of Light by Small Particles*. Wiley-Interscience, New York, 1983.
14. Stevens, T.D., "Bistatic Lidar Measurements of Lower Tropospheric Aerosols," Ph.D. Dissertation in Electrical Engineering, Penn State University, 1996.
15. Novitsky, Edward J., "Multistatic LIDAR Profile Measurements of Lower Tropospheric Aerosol and Particulate Matter," Ph.D. Dissertation in Electrical Engineering, Penn State University, 2002.
16. Novitsky, E. J., and C. R. Philbrick, "Multistatic Lidar Profiling of Urban Atmospheric Aerosols," *J. Geophys. Res* 110, D07S11, 1-11, 2005.